



Tarım Bilimleri Dergisi  
Tar. Bil. Der.

Dergi web sayfası:  
www.agri.ankara.edu.tr/dergi

Journal of Agricultural Sciences

Journal homepage:  
www.agri.ankara.edu.tr/journal

## Determination of Infrared Drying Characteristics and Modelling of Drying Behaviour of Carrot Pomace

İbrahim DOYMAZ<sup>a</sup>

<sup>a</sup>*Yildiz Technical University, Department of Chemical Engineering, Esenler, 34210, Istanbul, TURKEY*

### ARTICLE INFO

Research Article – Agricultural Technologies [https://doi.org/10.1501/Tarimbil\\_0000001227](https://doi.org/10.1501/Tarimbil_0000001227)

Corresponding Author: İbrahim DOYMAZ, E-mail: doymaz@yildiz.edu.tr, Tel: +90 (212) 383 47 48

Received: 03 January 2013, Received in Revised Form: 21 March 2013, Accepted: 15 April 2013

### ABSTRACT

In this study, drying characteristics of carrot pomace were determined and the applicability of different drying models was investigated in order to find the product's moisture content at any time of the drying process. Drying times of carrot pomace were found by drying at the infrared power levels of 83, 125, 167 and 209 W. It was observed that the power level affected the drying rate and time. To evaluate the drying kinetics of carrot pomace, the obtained experimental data were applied to twelve mathematical models and the model with the best fit was determined. According to the results, Aghbashlo et al model is superior to the others for explaining drying behavior of carrot pomace. Effective moisture diffusivity varied from 0.59 to  $3.40 \times 10^{-10} \text{ m}^2 \text{ s}^{-1}$  and was significantly influenced by infrared power. Activation energy was estimated by a modified Arrhenius type equation and found to be  $5.73 \text{ kW kg}^{-1}$ .

Keywords: Activation energy; Carrot pomace; Effective moisture diffusivity; Infrared drying; Mathematical modelling

## Havuç Posasının İnfrared Kurutma Karakteristiklerinin Belirlenmesi ve Kurutma Davranışının Modellenmesi

### ESER BİLGİSİ

Araştırma Makalesi – Tarım Teknolojileri

Sorumlu Yazar: İbrahim DOYMAZ, E-posta: doymaz@yildiz.edu.tr, Tel: +90 (212) 383 47 48

Geliş Tarihi : 03 Ocak 2013, Düzeltmelerin Gelişi: 21 Mart 2013, Kabul: 15 Nisan 2013

### ÖZET

Bu çalışmada, havuç posasının kurutma karakteristikleri belirlenmiş ve kuruma süresinin belirli bir anındaki ürünün nem içeriğinin bulunması için mevcut kurutma modellerinin uygulanabilirliği araştırılmıştır. Havuç posası 83, 125, 167 ve 209 W infrared güç seviyelerinde kurutulmuş kurutma süreleri bulunmuştur. Güç seviyesinin, kurutma hızına ve süresine etki ettiği gözlemlenmiştir. Havuç posasının kurutma kinetiğini belirlenmesi için, elde edilen deneysel veriler 12 adet matematiksel modele uygulanarak en uygun model belirlenmiştir. Elde edilen sonuçlara göre, Aghbashlo et al modelinin havuç posasının kuruma davranışını diğerlerinden daha iyi açıkladığı belirlenmiştir.

Efektif nem difüzyon hızları  $0.59$  ile  $3.40 \times 10^{-10} \text{ m}^2 \text{ s}^{-1}$  arasında değişmekte olup infrared güç seviyesinden önemli şekilde etkilenmektedir. Arrhenius tip modeli ile aktivasyon enerjisi hesaplanmış ve  $5.73 \text{ kW kg}^{-1}$  olarak bulunmuştur.

Anahtar Kelimeler: Aktivasyon enerjisi; Havuç posası; Efektif nem difüzyon hızı; İnfrared kurutma; Matematiksel modelleme

## 1. Introduction

The carrot is one of the popular root vegetables grown throughout the world. The edible part of carrot, which is eaten as raw, converted to juice drink, used as salads, cooked as vegetable dish, is used to make sweet dishes (Kumar et al 2012). Carrot highly nutritious as it contains appreciable amount of vitamins B1, B2, B6 and B12. It is also contains many important minerals. Moreover, carrots have the highest  $\beta$ -carotene content among human foods (Eim et al 2011). Carrots are processed into products such as canned, dried, juice, beverages, candy, preserves and intermediate moisture products (Sharma et al 2012).

By-products, wastes and pomaces of food processing, which represent a major disposal problem for the industry concerned, are very promising sources of value-added substances (Vega-Gálvez et al 2010). Many agricultural by-products are commonly used as animal feeds or fertilizers. Carrot juice sector generates large quantities of carrot pomace. This caused serious environmental pollution as well as acting as a substrate for insect and microbial proliferation. The processed carrot pomace have generally high moisture contents (about 89.17%, w.b.), and need to removal of moisture before the production of high-added value products. Efforts have been made to utilize carrot pomace in foods such as bread, cake, dressing, pickle, preparation of high fibre biscuits and production of functional drinks (Sharma et al 2012). Drying has always been of great importance to the preservation of agricultural products and by-products.

Drying is one of the oldest methods of food preservation as well as an important food processing. The removal of moisture prevents

the growth and reproduction of microorganisms which cause decay, and minimises many of the moisture-mediated deteriorative reactions. It brings about substantial reduction in weight and volume, minimizing packing, storage and transportation costs and enables storability of the product under ambient temperatures (Brooks et al 2008; Demir & Saçılık 2010). Drying is the most energy intensive process in food industry. Therefore, new drying techniques and dryers must be designed and studied to minimize the energy cost in drying process (Kocabıyık & Tezer 2009).

Infrared drying has gained popularity as an alternative drying method for a variety of agricultural products. When infrared radiation is used to heat or dry moist materials, penetrates it and the energy of radiation converts into heat. When a material is exposed to infrared radiation, both the surface and the inner layers are heated intensely, resulting in a high rate of heat and mass transfer compared with conventional drying (Hebbbar & Ramesh 2005). The use of infrared radiation technology in drying agricultural products has several advantages. These may include decreased drying time, high energy efficiency, high quality finished products, and uniform temperature in the product (Nowak & Lewicki 2004; Sharma et al 2005). Several agricultural products and by-products have been successfully dried by the infrared application and/or by a combined infrared-assisted convection process such as onion (Sharma et al 2005), apple pomace (Sun et al 2007), seedless grapes (Çağlar et al 2009), red pepper (Nasıroğlu & Kocabıyık 2009), carrot (Kocabıyık & Tezer 2009), grape by-products (Ruiz Celma et al 2009a), and tomato by-products (Ruiz Celma et al 2009b). So far, there is no information available about infrared drying of carrot pomace. The main objectives of this study were to

investigate the effect of infrared power levels on the drying rate and time, fit the experimental data to twelve mathematical models, and compute effective diffusivity and activation energy of carrot pomace.

## 2. Material and Methods

### 2.1. Material

Fresh carrots (*Daucus carota* L.) were obtained from a local supermarket and stored at 4°C until analysis. For samples preparation, the carrots were washed with cold water, dripped and peeled. In this study, carrot pomace (peel) was used. The initial and final moisture contents of carrot pomace were determined by using the oven method at 110°C for 24 h (Alibaş 2012). Triplicate samples were used for the determination of moisture content and the average values were reported as 8.233 kg water kg<sup>-1</sup> dm (d.b.)

### 2.2. Drying procedure

Drying experiments were carried out in a moisture analyzer with one 250 W halogen lamp (Snijders Moisture Balance, Snijders b.v., Tilburg, Holland). In infrared drying process, the sample should be separated evenly and homogeneously over the entire pan. Otherwise, a large portion of the incident infrared radiation will be reflected at the exposed pan bottom not covered by the sample (Çağlar et al 2009). The experiments were performed at infrared power levels varying from 83 to 209 W. The power level was set in control unit of equipment. Moisture loss in the samples with initial load of 40±0.2 g and thickness of about 10±1 mm was measured with a digital balance (Mettler-Toledo AG, Grefensee, Switzerland, model BB3000) with accuracy of 0.1 g and recorded at 10 min intervals. The experiments ended at the point of reading constant weight (about 0.015 kg water kg<sup>-1</sup> dm (d.b.)). The dried product was cooled and packed in low-density polyethylene bags that were heat-sealed. All experiments were conducted in duplicate and the average of the moisture content at each value was used for drawing the drying curves.

### 2.3. Mathematical modelling

The data derived from drying of carrot pomace was fitted with twelve drying models typically used for the modeling of drying curves (Table 1). The moisture ratio (*MR*) of the samples is determined by the following equation (Alibaş 2012):

$$MR = \frac{M_t - M_e}{M_0 - M_e} \quad (1)$$

Where  $M_t$ ,  $M_0$  and  $M_e$  are the moisture content at any time, initial moisture content, and equilibrium moisture content, kg water kg<sup>-1</sup> dm, respectively, and  $t$  is the drying time, min.

The moisture ratio (*MR*) was simplified to  $M_t/M_0$  instead of  $(M_t - M_e)/(M_0 - M_e)$  by some investigators (Dissa et al 2011; Montero et al 2011) because of the values of  $M_e$  small compared with  $M_t$  or  $M_0$  for long drying time.

The drying rate (*DR*) of carrot pomace was calculated using the following equation (Evin 2012):

$$DR = \frac{M_t - M_{t+\Delta t}}{\Delta t} \quad (2)$$

Where  $M_{t+\Delta t}$  is the moisture content at  $t+\Delta t$ , kg water kg<sup>-1</sup> dm;  $t$  is the time, min.

### 2.4. Statistical analysis

Data were analyzed using Statistica 6.0 (StatSoft Inc., USA) software package. The parameters of models were estimated using a non-linear regression procedure based on the Levenberg-Marquardt algorithm. The fitting quality of the experimental data to all models was evaluated using the coefficient of determination ( $R^2$ ), mean relative percent error ( $P$ ), reduced chi-square ( $\chi^2$ ) and root mean square error ( $RMSE$ ). These parameters were calculated from the following formulas:

$$R^2 = 1 - \frac{\sum (MR_{pre,i} - MR_{exp,j})^2}{\sum_{i=1}^N (\overline{MR}_{pre} - MR_{exp,j})^2} \quad (3)$$

**Table 1- Mathematical models applied to the drying curves**

Çizelge 1- Kurutma eğrileri için uygulanan modeller

Model name	Model	Reference
Lewis	$MR = \exp(-kt)$	Roberts et al (2008)
Henderson and Pabis	$MR = a \exp(-kt)$	Erbay and Icier (2010)
Logarithmic	$MR = a \exp(-kt) + c$	Wang et al (2007)
Two-term	$MR = a \exp(-k_0t) + b \exp(-k_1t)$	Zielinska and Markowski (2010)
Approximation of diffusion	$MR = a \exp(-kt) + (1 - a) \exp(-kbt)$	Dissa et al (2011)
Verma et al	$MR = a \exp(-kt) + (1 - a) \exp(-gt)$	Verma et al (1985)
Page	$MR = \exp(-kt^n)$	Sun et al (2007)
Midilli et al	$MR = a \exp(-kt^n) + bt$	Ruiz Celma et al (2009b)
Parabolic	$MR = a + bt + ct^2$	Sharma and Prasad (2004)
Wang and Singh	$MR = 1 + at + bt^2$	Akpınar (2010)
Weibull	$MR = \exp\left(-\left(\frac{t}{b}\right)^a\right)$	Corzo et al (2010)
Aghbashlo et al	$MR = \exp\left(-\frac{k_1t}{1 + k_2t}\right)$	Aghbashlo et al (2009)

$$P = \frac{100}{N} \sum_{i=1}^N \frac{|MR_{exp,i} - MR_{pre,i}|}{MR_{exp,i}} \quad (4)$$

$$\chi^2 = \frac{\sum_{i=1}^N (MR_{exp,i} - MR_{pre,i})^2}{N - z} \quad (5)$$

$$RMSE = \left[ \frac{1}{N} \sum_{i=1}^N (MR_{pre,i} - MR_{exp,i})^2 \right]^{1/2} \quad (6)$$

Where  $MR_{exp,i}$  and  $MR_{pre,i}$  are the experimental and predicted dimensionless moisture ratios, respectively;  $N$  is the number of observations;  $z$  is the number of constants.

The best model describing the drying characteristics of samples was chosen as the one with the highest  $R^2$ , the least  $P$ ,  $\chi^2$  and  $RMSE$  (Çağlar et al 2009; Ruiz Celma et al 2009a; Kayışoğlu & Ertekin 2011; Alibaş 2012).

### 2.5. Determination of effective diffusivity

The effective moisture diffusivity is an important transport property in food and other materials drying processes modelling, being a function of temperature and moisture content in material. Fick's second law of diffusion equation, symbolized as a mass-diffusion equation for drying of agricultural products in a falling rate period, is shown in the following equation:

$$\frac{\partial M}{\partial t} = D_{eff} \nabla^2 M \quad (7)$$

The solution of diffusion equation (Equation 7) for slab geometry is solved by Crank (1975), and supposed uniform initial moisture distribution, negligible external resistance, constant diffusivity and negligible shrinkage:

$$MR = \frac{8}{\pi^2} \left[ \exp\left(-\frac{\pi^2 D_{eff} t}{4L^2}\right) + \frac{1}{9} \exp\left(-9 \frac{\pi^2 D_{eff} t}{4L^2}\right) + \frac{1}{25} \exp\left(-25 \frac{\pi^2 D_{eff} t}{4L^2}\right) + \dots \right] \quad (8)$$

Where  $D_{eff}$  is the effective moisture diffusivity,  $m^2 s^{-1}$ ;  $t$  is the drying time,  $s$ ;  $L$  is the half-thickness of samples,  $m$ ;  $n$  is a positive integer.

For long drying times, Equation 8 simplifies to a limiting form of the diffusion equation as given by Equation 9:

$$MR = \frac{8}{\pi^2} \exp\left(-\frac{\pi^2 D_{eff} t}{4L^2}\right) \quad (9)$$

From Equation 9, a plot of  $\ln MR$  versus drying time should give a straight line with a slope ( $K$ ):

$$K = \frac{\pi^2 D_{eff}}{4L^2} \quad (10)$$

Using the slope value (Equation 10), the effective moisture diffusivity could be determined.

### 2.6. Determination of activation energy

Temperature is not directly measurable quantity in the infrared power level during drying process in this study. For the calculation of activation energy, modified form of Arrhenius equation as derived by Dadalı and Özbek (2008) show the relationship between the effective diffusivity and the infrared power level to sample weight.

$$D_{eff} = D_0 \exp\left(-\frac{E_a m}{p}\right) \quad (11)$$

Where  $D_0$  is the pre-exponential factor of Arrhenius equation ( $m^2 s^{-1}$ ),  $E_a$  is the activation energy ( $W kg^{-1}$ ),  $p$  is the infrared power level ( $W$ ), and  $m$  is the sample weight ( $kg$ ).

## 3. Results and Discussion

### 3.1. Drying curves

The effects of infrared power on moisture content with drying time and drying rate versus drying time are shown in Figure 1. According to the results in

Figure 1, the infrared power level had a significant effect on the moisture content of the carrot pomace as expected. The results showed that drying time decreased greatly when the infrared power level increased. The drying time required to reach the final moisture content of samples were 310, 160, 100 and 60 min at the infrared power levels of 83, 125, 167 and 209 W, respectively. The average drying rates increased 5.16 times as infrared power level increased from 83 W to 209 W. The decrease in drying time with an increase in the infrared power level has been reported by Kocabıyık and Tezer (2009) for carrot slices, Sharma et al (2005) for onion slices, and Nasıroğlu and Kocabıyık (2009) for red pepper slices.

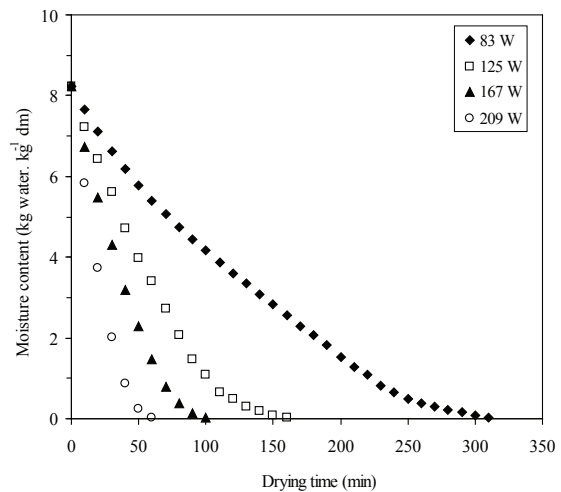


**Figure 1- Drying curves of carrot pomace at different power levels**

*Şekil 1- Farklı güç seviyelerinde havuç posasının kurutma eğrileri*

### 3.2. Drying rate

The drying rate curves of carrot pomace are shown in Figure 2. It is clear that the drying rate decrease continuously with moisture content. As can be seen in Figure 2, a constant-rate period was not observed in infrared drying of the carrot pomace samples. The drying process occurred entirely in the falling-rate period. This shows that diffusion is dominant physical mechanism governing moisture movement in the samples. During drying, the drying rates were

higher in the beginning of the process, and after that decreased with decrease of moisture content in the samples. The reason for reduction of drying rate might due to reduction in porosity of samples due to shrinkage with advancement of drying process, which increased the resistance to movement of water leading to further fall in drying rates (Singh et al 2006). This observation is in agreement with previous studies on infrared drying of food by-products (Sun et al 2007; Ruiz Celma et al 2009a, b; Vega-Gálvez et al 2010).

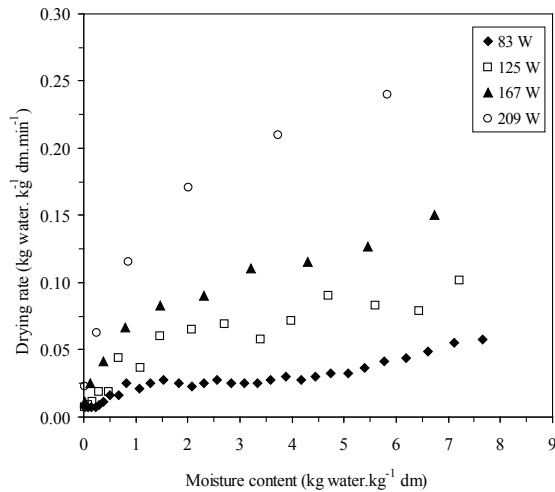


**Figure 2- Drying rate curves of the carrot pomace at different power levels**

*Şekil 2- Farklı güç seviyelerinde havuç posasının kurutma hızı eğrileri*

**3.3. Fitting of the drying curves**

An efficient modelling of the falling rate period is highly relevant task in a drying process (Ruiz Celma et al 2009b). For that purpose, a wide set of thin-layer drying models were examined in the present work. The selected models are identified in Table 1. The best model selected based on the highest  $R^2$  and the lowest  $P$ ,  $\chi^2$  and  $RMSE$  values. Results of the statistical computing are shown in Table 2. The  $R^2$  values for all models were above 0.94, and that for Lewis and Henderson and Pabis models were lower. The statistical parameter estimations showed that  $R^2$ ,  $P$ ,  $\chi^2$  and  $RMSE$  values were ranged from 0.9463 to 0.9999, 6.6091 to 499.2718, 0.000001 to 0.005682,

and 0.002315 to 0.375065, respectively. Among the twelve models, the Aghbashlo et al model fitted the best with experimental drying data for carrot pomace, with the highest  $R^2$  for all power levels. The  $P$ ,  $\chi^2$  and  $RMSE$  also showed best results with the smaller values. It is clear that, the  $R^2$ ,  $P$ ,  $\chi^2$  and  $RMSE$  values of this model were changed between 0.9995-0.9999, 6.6091-20.4859, 0.000001-0.000050 and 0.002315-0.028593, respectively. The Aghbashlo et al (2009) model constants of  $k_1$  and  $k_2$  were regressed against the drying variables using multiple regression analysis, and the Equations 12 and 13 were resulted:

$$k_1 = 1.10 \cdot 10^{-6} p^2 - 0.0001 p + 0.0087 \quad (R^2: 0.994) \quad (12)$$

$$k_2 = -3 \cdot 10^{-7} p^2 - 5 \cdot 10^{-5} p - 0.0008 \quad (R^2: 0.992) \quad (13)$$

The accuracy of the established model was evaluated by comparing the predicted moisture ratios with the observed values as shown in Figure 3. The closeness of the plotted data to the straight line representing equality between the experimental and predicted values illustrates by the best suitability of Aghbashlo et al model for describing the drying characteristics of carrot pomace.

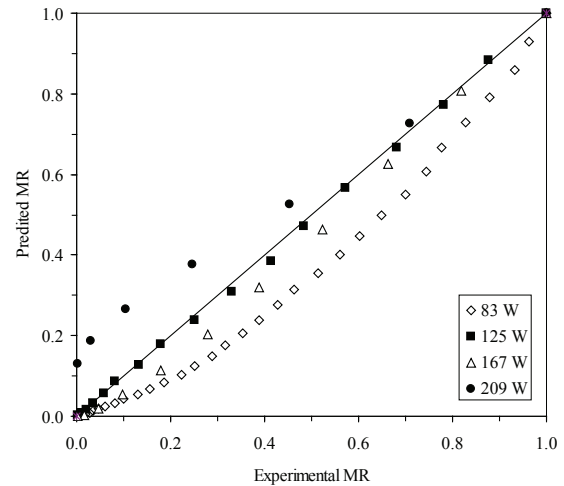


**Figure 3- Comparing moisture ratio values of experimental versus predicted by Aghbashlo et al model during carrot pomace drying at different power levels**

*Şekil 3- Farklı güç seviyelerinde havuç posasının kurutulması sırasında deneysel ile Aghbashlo et al modelinin tahmini nem oranlarının karşılaştırılması*



**Table 2- Statistical analysis of models at various infrared power levels***Çizelge 2- Farklı infrared güç seviyelerinde modellerin istatistiksel analizi*

Model	$p$ (W)	Model constants and coefficients	$R^2$	$P$	$\chi^2$	RMSE
Lewis	83	k: 0.0074	0.9463	256.7793	0.005682	0.375065
	125	k: 0.0171	0.9675	282.1346	0.003552	0.217281
	167	k: 0.0263	0.9703	403.4656	0.003532	0.167082
	209	k: 0.0461	0.9759	499.2718	0.003419	0.121404
Henderson and Pabis	83	a: 1.1222, k: 0.0083	0.9635	216.5240	0.003993	0.303593
	125	a: 1.0755, k: 0.0183	0.9742	248.8876	0.003011	0.198501
	167	a: 1.0591, k: 0.0277	0.9749	368.9009	0.003317	0.159155
	209	a: 1.0042, k: 0.0478	0.9785	469.7338	0.003670	0.124960
Logarithmic	83	a: 1.5314, k: 0.0039, c: -0.4875	0.9963	88.7449	0.000415	0.090838
	125	a: 1.2544, k: 0.1171, c: -0.2289	0.9952	142.8944	0.000592	0.082229
	167	a: 1.2789, k: 0.0170, c: -0.2637	0.9971	164.9706	0.000427	0.048792
	209	a: 1.2213, k: 0.0320, c: -0.2056	0.9962	225.2664	0.000800	0.053571
Two-term	83	a: 6.0143, b: -4.9712, $k_0$ : 0.0026, $k_1$ : 0.0019	0.9966	82.2950	0.000389	0.085920
	125	a: 37.6068, b: -36.6305, $k_0$ : 0.0324, $k_1$ : 0.0332	0.9941	120.1738	0.000786	0.090870
	167	a: 53.0503, b: -52.0641, $k_0$ : 0.0493, $k_1$ : 0.0501	0.9937	193.2523	0.001064	0.078299
	209	a: 33.8938, b: -34.8906, $k_0$ : 0.0897, $k_1$ : 0.0875	0.9968	208.2060	0.000889	0.047124
Approximation of diffusion	83	a: -13.4191, k: 0.0158, b: 0.9335	0.9918	118.1879	0.000924	0.144804
	125	a: -14.8193, k: 0.0332, b: 0.9477	0.9937	123.7434	0.000779	0.090255
	167	a: -16.4714, k: 0.0505, b: 0.9536	0.9935	195.0935	0.000957	0.075869
	209	a: -16.2039, k: 0.0908, b: 0.9499	0.9966	208.6709	0.000670	0.046126
Verma et al	83	a: -10.8683, k: 0.0159, g: 0.0247	0.9918	118.2895	0.000926	0.144882
	125	a: 0.1331, k: 0.0171, g: 0.0171	0.9675	282.0247	0.004059	0.217273
	167	a: 0.1890, k: 0.0263, g: 0.0263	0.9703	403.4855	0.004414	0.167080
	209	a: 4.6844, k: 0.0209, b: 0.0166	0.9966	211.3269	0.000711	0.046405
Page	83	k: 0.0005, n: 1.5301	0.9958	80.7114	0.000509	0.107935
	125	k: 0.0032, n: 1.3908	0.9951	90.5672	0.000567	0.077919
	167	k: 0.0063, n: 1.3762	0.9948	153.1934	0.000688	0.069102
	209	k: 0.0124, n: 1.4010	0.9979	154.7671	0.000358	0.037380
Midilli et al	83	a: 0.9874, b: -0.0003, k: 0.0008, n: 1.3955	0.9992	35.9849	0.000088	0.041345
	125	a: 0.9796, b: -0.0003, k: 0.0032, n: 1.3198	0.9981	62.6047	0.000254	0.048890
	167	a: 0.9907, b: -0.0008, k: 0.0092, n: 1.2341	0.9986	92.8046	0.000235	0.035610
	209	a: 0.9974, b: -0.0007, k: 0.0159, n: 1.2995	0.9994	75.3408	0.000169	0.020756
Parabolic	83	a: 1.0385, b: -0.0056, c: 0.0000	0.9981	48.7654	0.000211	0.061297
	125	a: 1.0105, b: -0.0126, c: 0.0000	0.9990	20.2011	0.000123	0.035192
	167	a: 1.0044, b: -0.0190, c: 0.0000	0.9996	39.8121	0.000057	0.019191
	209	a: 1.0068, b: -0.0335, c: 0.0003	0.9997	17.1091	0.000061	0.014330
Wang and Singh	83	a: -0.0051, b: 0.0000	0.9963	72.6790	0.000403	0.094517
	125	a: -0.0123, b: 0.0000	0.9988	29.8122	0.000132	0.036897
	167	a: -0.0189, b: 0.0001	0.9995	44.6024	0.000054	0.018369
	209	a: -0.0331, b: 0.0002	0.9996	25.0631	0.000062	0.014168
Weibull	83	a: 1.5301, b: 140.1561	0.9953	80.7074	0.000509	0.107935
	125	a: 1.3908, b: 61.2475	0.9951	90.5656	0.000567	0.077918
	167	a: 1.3762, b: 39.7589	0.9979	153.1973	0.000686	0.069102
	209	a: 1.4010, b: 22.8523		154.7625	0.000358	0.037380
Aghbashlo et al	83	$k_1$ : 0.0043, $k_2$ : 0.0024	0.9995	7.5951	0.000048	0.028593
	125	$k_1$ : 0.0112, $k_2$ : 0.0044	0.9995	6.6091	0.000050	0.020204
	167	$k_1$ : 0.0174, $k_2$ : 0.0066	0.9997	20.4859	0.000037	0.014896
	209	$k_1$ : 0.0306, $k_2$ : 0.0114	0.9999	8.9979	0.000001	0.002315

### 3.4. Effective moisture diffusivity

The values of effective moisture diffusivity were calculated using Equation 10 and are shown in Figure 4. The  $D_{eff}$  values of carrot pomace in the infrared drying process at 83-209 W varied in the range of  $0.59-3.40 \times 10^{-9} \text{ m}^2 \text{ s}^{-1}$ . It can be seen that  $D_{eff}$  values increased greatly with increasing infrared power level. Drying at 209 W has the highest value of effective moisture diffusivity and the lowest value was obtained for 83 W. The values of  $D_{eff}$  from this study lie within in general range  $10^{-12}$  to  $10^{-8} \text{ m}^2 \text{ s}^{-1}$  for drying of food materials (Zogzas et al 1996). As expected, the values of  $D_{eff}$  increased with the increase of output power. This result is similar to the results for carrot pomace (Kumar et al 2012), apple pomace (Sun et al 2007), and tomato by-products (Ruiz Celma et al 2009b). The effect of infrared power on effective diffusivity is defined by the following equation:

$$D_{eff} = 4 \times 10^{-11} p - 4 \times 10^{-9} \quad (R^2 = 0.9955) \quad (14)$$

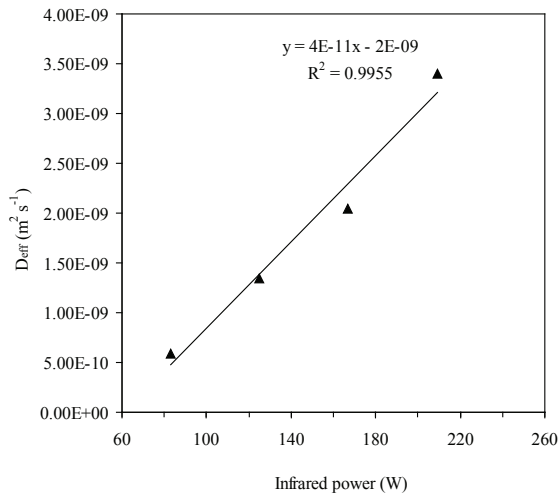


**Figure 4- Variation of effective moisture diffusivity with power level**

Şekil 4- Efektif nem diffüzyivitesinin güç seviyesi ile değişimi

### 3.5. Activation energy

The activation energy can be determined from the slope of Arrhenius plot,  $\ln(D_{eff})$  versus  $m/p$

(Equation 11). The  $\ln(D_{eff})$  as a function of the sample weight/infrared power level was plotted in Figure 5. The slope of the line is  $(-E_a)$  and the intercept equals to  $\ln(D_0)$ . The results show a linear relationship due to Arrhenius type dependence. Equation 15 shows the effect of sample weight/power level on  $D_{eff}$  of samples with the following coefficients:

$$D_{eff} = 8.9734 \times 10^{-9} \exp\left(-\frac{5729.6 \text{ m}}{p}\right) \quad R^2 = 0.9791 \quad (15)$$

The estimated values of  $D_0$  and  $E_a$  from modified Arrhenius type exponential Equation 15 are  $8.9734 \times 10^{-9} \text{ m}^2 \text{ s}^{-1}$  and  $5.73 \text{ kW kg}^{-1}$ , respectively.

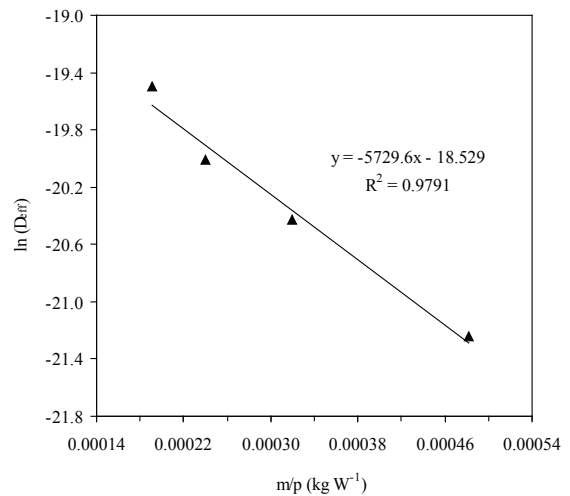


**Figure 5- Arrhenius-type relationship between effective moisture diffusivity and power level**

Şekil 5- Efektif nem diffüzyivitesi ile güç seviyesi arasındaki Arrhenius tip ilişkisi

## 4. Conclusions

Based on the results of this study, the following conclusions were drawn:

- As the infrared power level increases, drying rate increases and drying time decreases.
- A constant-rate period was not observed in the infrared drying of carrot pomace; all the drying process occurred in the falling-rate drying period.



- The Aghbashlo et al model gave the best representations of drying data under all experimental conditions.
- The effective moisture diffusivity varied between  $0.59$  and  $3.40 \times 10^{-10} \text{ m}^2 \text{ s}^{-1}$  and increases as infrared power increases.
- Activation energy was estimated by a modified Arrhenius type equation and found to be  $5.73 \text{ kW kg}^{-1}$ .

### Abbreviations and Symbols

$a, b, c, g, n$	Empirical constants in drying models
$D_{eff}$	Effective diffusivity, $\text{m}^2 \text{ s}^{-1}$
$D_0$	Pre-exponential factor, $\text{m}^2 \text{ s}^{-1}$
$E_a$	Activation energy, $\text{W kg}^{-1}$
$K$	Slope
$k, k_0, k_1, k_2$	Empirical coefficients in the drying models, $\text{min}^{-1}$
$M$	Moisture content at any time, $\text{kg water kg}^{-1} \text{ dm}$
$M_e$	Equilibrium moisture content, $\text{kg water kg}^{-1} \text{ dm}$
$M_0$	Initial moisture content, $\text{kg water kg}^{-1} \text{ dm}$
$MR$	Moisture ratio
$N$	Number of observations
$n$	Positive integer
$R^2$	Coefficient of determination
$RMSE$	Root mean square error
$T$	Temperature, $^{\circ}\text{C}$
$t$	Drying time, $\text{min}$
$z$	Number of constants
$\chi^2$	Reduced chi-square

### References

Alibaş İ (2012). Asma yaprağının (*Vitis vinifera* L.) mikrodalga enerjisiyle kurutulması ve bazı kalite parametrelerinin belirlenmesi. *Tarım Bilimleri Dergisi-Journal of Agricultural Sciences* **18**: 43-53

Aghbashlo M, Kianmehr M H, Khani S & Ghasemi M (2009). Mathematical modeling of carrot thin-layer drying using new model. *International Agrophysics* **23**: 313-317

Akpınar E K (2010). Drying of mint leaves in a solar dryer and under open sun: Modelling, performance analyses. *Energy Conversion and Management* **51**: 2407-2418

Brooks M S, Abou El-Hana N H & Ghaly A E (2008). Effects of tomato geometries and air temperature on the drying behaviour of plum tomato. *American Journal of Applied Sciences* **5**: 1369-1375

Çağlar A, Toğrul I T & Toğrul H (2009). Moisture and thermal diffusivity of seedless grape under infrared drying. *Food and Bioproducts Processing* **87**: 292-300

Corzo O, Bracho N, Pereira A. & Vásquez A (2008). Weibull distribution for modelling air drying of coroba slices. *LWT - Food Science and Technology* **41**: 2023-2028

Crank J (1975). *The Mathematics of Diffusion*, second ed. Oxford University Press, London, UK

Dadalı G & Özbek B (2008). Microwave heat treatment of leek: drying kinetic and effective moisture diffusivity. *International Journal of Food Science and Technology* **43**: 1443-1451

Demir K & Saçılık, K (2010). Solar drying of Ayaş tomato using a natural convection solar tunnel dryer. *Journal of Food, Agriculture and Environment* **8** (1): 7-12

Dissa A O, Bathiebo D J, Desmorieux H, Coulibaly O & Kouliadiati J (2011). Experimental characterization and modelling of thin layer direct solar drying of *Amelia* and *Brooks* mangoes. *Energy* **36**: 2517-2527

Eim V S, Rosselló C, Femenia A A & Simal S (2011). Moisture sorption isotherms and thermodynamic properties of carrot. *International Journal Food Engineering* **7** (3): Article 13

Erbay Z & Icier F (2010). Thin-layer drying behaviours of olive leaves (*Olea Europaea* L.). *Journal of Food Process Engineering* **33**: 287-308

Evin D (2012). Thin layer drying kinetics of *Gundelia tournefortii* L. *Food and Bioproducts Processing* **90**: 323-332

Hebbar U H & Ramesh M N (2005). Optimisation of processing conditions for infrared drying of cashew kernels with taste. *Journal of the Science of Food and Agriculture* **85**: 865-871

- Kayısoğlu S & Ertekin C (2011). Vacuum drying kinetics of Barbunya bean (*Phaseolus vulgaris* L. *elipticus* Mart.). *Philippine Agricultural Scientist* **94**: 285-291
- Kocabiyık H & Tezer D (2009). Drying of carrot slices using infrared radiation. *International Journal of Food Science and Technology* **44**: 953-959
- Kumar N, Sarkar B C & Sharma H K (2012). Mathematical modelling of thin layer hot air drying of carrot pomace. *Journal of Food Science and Technology* **17**: 33-41
- Montero I, Miranda T, Arranz J I & Rojas C V (2011). Thin layer drying kinetics of by-products from olive oil processing. *International Journal of Molecular Sciences* **12**: 7885-7897
- Nasiroğlu S & Kocabiyık H (2009). Thin-layer infrared radiation drying of red pepper slices. *Journal of Food Process Engineering* **32**: 1-16
- Nowak D & Lewicki P P (2004). Infrared drying of apple slices. *Innovative Food Science & Emerging Technology* **5**: 353-360
- Roberts J S, Kidd D R & Padilla-Zakour O (2008). Drying kinetics of grape seeds. *Journal of Food Engineering* **89**: 460-465
- Ruiz Celma A, López-Rodríguez F & Cuadros Blázquez F (2009a). Experimental modelling of infrared drying of industrial grape by-products. *Food and Bioproducts Processing* **87**: 247-253
- Ruiz Celma A, Cuadros Blázquez F & López-Rodríguez F (2009b). Experimental characterisation of industrial tomato by-products from infrared drying process. *Food and Bioproducts Processing* **87**: 282-291
- Sharma K D, Karki S, Thakur N S & Attri S (2012). Chemical composition, functional properties and processing of carrot – a review. *Journal of Food Science and Technology* **49**: 22-32
- Sharma G P & Prasad S (2004). Effective moisture diffusivity of garlic cloves undergoing microwave-convective drying. *Journal of Food Engineering* **65**: 609-617
- Sharma G P, Verma R C & Pathare P B (2005). Thin-layer infrared radiation drying of onion slices. *Journal of Food Engineering* **67**: 361-366
- Singh B, Panesar PS & Nanda V (2006). Utilization of carrot pomace for the preparation of a value added product. *World Journal of Dairy Food Science* **1**(1): 22-27
- Sun J, Hu X, Zhao G, Wu J, Wang Z, Chen F & Liao X (2007). Characteristics of thin-layer infrared drying of apple pomace with and without hot air pre-drying. *Food Science and Technology International* **13**(2): 91-97
- Vega-Gálvez A, Miranda M, Diaz L P, Lopez L, Rodriguez K & Di Scala K (2010). Effective moisture diffusivity determination and mathematical modelling of the drying curves of the olive-waste cake. *Bioresource Technology* **101**: 7265-7270
- Verma L R, Bucklin R A, Endan J B & Wratten F T (1985). Effects of drying air parameters on rice drying models. *Transaction of ASAE* **28**: 296-301
- Wang Z, Sun J, Liao X, Chen F, Zhao G, Wu J & Hu X (2007). Mathematical modeling on hot air drying of thin layer apple pomace. *Food Research International* **40**:39-46
- Zielinska M & Markowski M (2010). Air drying characteristics and moisture diffusivity of carrots. *Chemical Engineering and Processing* **49**: 212-218
- Zogzas N P, Maroulis Z B & Marinos-Kouris D (1996). Moisture diffusivity data compilation in foodstuffs. *Drying Technology* **14**: 2225-2253